Journal of Medicinal Chemistry

Article

pubs.acs.org/jmc

Discovery of *Mycobacterium tuberculosis* InhA Inhibitors by Binding Sites Comparison and Ligands Prediction

Tanja Štular,[†] Samo Lešnik,[†] Kaja Rožman,[‡] Julia Schink,[§] Mitja Zdouc,[§] An Ghysels,[∥] Feng Liu,[⊥] Courtney C. Aldrich,[#] V. Joachim Haupt,[▽] Sebastian Salentin,[▽] Simone Daminelli,[▽] Michael Schroeder,[▽] Thierry Langer,[○] Stanislav Gobec,[‡] Dušanka Janežič,[*,§] and Janez Konc[*,†,§]

[†]National Institute of Chemistry, Hajdrihova 19, SI-1000 Ljubljana, Slovenia

[‡]Faculty of Pharmacy, University of Ljubljana, Aškerčeva cesta 7, SI-1000 Ljubljana, Slovenia

[§]Faculty of Mathematics, Natural Sciences and Information Technologies, University of Primorska, Glagoljaška 8, SI-6000 Koper, Slovenia

[∥]Center for Molecular Modeling, Ghent University, Technologiepark 903, 9052 Zwijnaarde, Belgium

[⊥]AAT Bioquest, Inc., 520 Mercury Drive, Sunnyvale, California 94085, United States

[#]Department of Medicinal Chemistry, University of Minnesota, 308 Harvard Street Southeast, Minneapolis, Minnesota 55455, United States

[▽]Biotechnology Center (BIOTEC), Technische Universität Dresden, 01307 Dresden, Germany

[○]Department of Pharmaceutical Chemistry, Faculty of Life Sciences, University of Vienna, Althanstrasse 14, A-1090 Vienna, Austria

Supporting Information

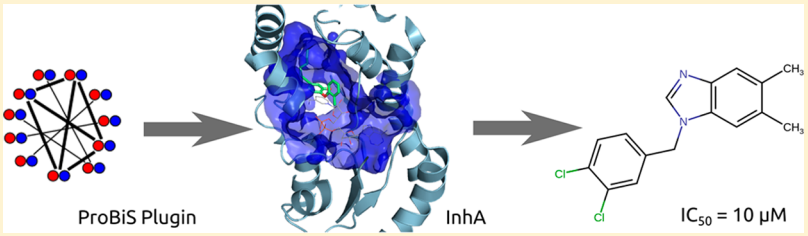

ABSTRACT: Drug discovery is usually focused on a single protein target; in this process, existing compounds that bind to related proteins are often ignored. We describe ProBiS plugin, extension of our earlier ProBiS-ligands approach, which for a given protein structure allows prediction of its binding sites and, for each binding site, the ligands from similar binding sites in the Protein Data Bank. We developed a new database of precalculated binding site comparisons of about 290000 proteins to allow fast prediction of binding sites in existing proteins. The plugin enables advanced viewing of predicted binding sites, ligands' poses, and their interactions in three-dimensional graphics. Using the InhA query protein, an enoyl reductase enzyme in the *Mycobacterium tuberculosis* fatty acid biosynthesis pathway, we predicted its possible ligands and assessed their inhibitory activity experimentally. This resulted in three previously unrecognized inhibitors with novel scaffolds, demonstrating the plugin's utility in the early drug discovery process.

INTRODUCTION

The number of structures in the Protein Data Bank (PDB)[1] continuously increases, and these structures are invaluable in the structure-based drug discovery process.[2−4] Identification of protein binding sites is a prerequisite in many applications including molecular docking[5] and de novo drug design.[6,7] Structural identification and comparison of functional sites is a necessary part of protein function prediction[8] and drug repositioning.[9−14]

Virtual screening is a widely used method in computer-aided drug discovery[15] which predicts molecules with high binding affinity to a target protein.[16] It supports the early stage identification of lead compounds, and inverse virtual screening[17] evaluates a single compound (e.g., a potential drug) against many proteins, searching for receptors that bind the given ligand with high affinity and predicting its secondary, or off-targets. Both virtual screening and its inverse counterpart have important roles in the drug discovery process.

Drug repositioning and ligand homology modeling methods,[18−22] developed as alternative means of virtual screening, have been successfully used in drug discovery.[23] These methods explicitly use information about existing ligands to construct and optimize new ligands for a given binding site. Ligands that bind to similar binding sites contain a set of functional groups and regions that are responsible for their binding and, in

Received: August 23, 2016
Published: November 29, 2016

DOI: 10.1021/acs.jmedchem.6b01277
J. Med. Chem. 2016, 59, 11069−11078

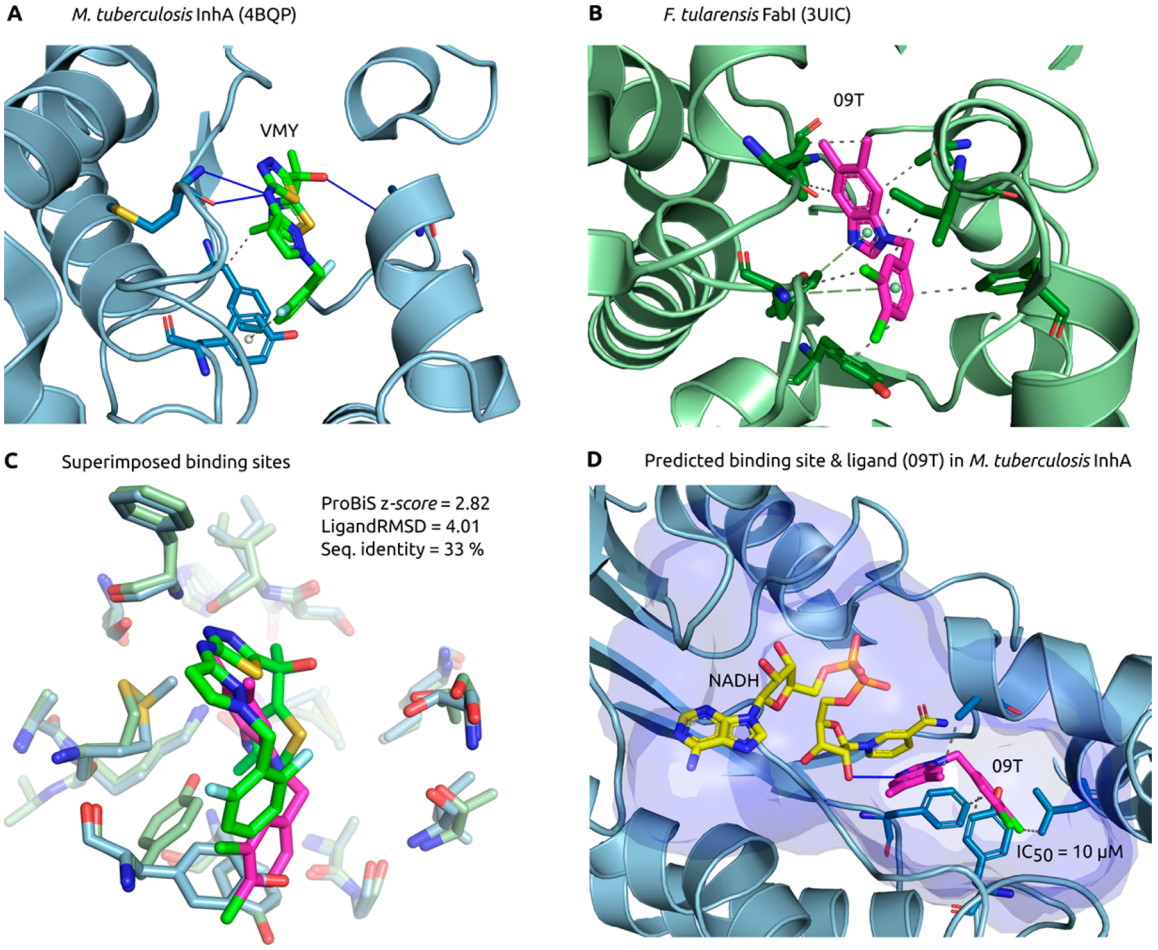

Figure 1. Prediction of ligands by binding site alignment using ProBiS plugin. The binding sites of the query *M. tuberculosis* InhA protein (A, blue) and of *F. tularensis* FabI protein (B, green) were aligned (C). On the basis of this alignment, the ligand of FabI was repositioned to InhA: predicted pose of the repositioned inhibitor (compound **4**; ligand ID: 09T)[40] in the InhA binding site (D, magenta sticks model); predicted binding site surface (blue transparent surface) is a union of volumes of all predicted ligands for InhA (only one ligand is shown). Interactions between the ligands and proteins: hydrogen bonds (blue solid lines), hydrophobic (dashed lines), π-stacking interactions (sphere in aromatic ring and dashed lines).

particular, for their specificity. Ligands that bind to a given binding site can sometimes be effective in one or more similar binding sites.

The ProBiS plugin described in this paper provides template ligands from different but similar crystal structures. Prediction of binding sites is accomplished by the ProBiS algorithm,[24] which compares a query protein to a database of existing small-ligand binding sites and detects structurally similar sites by matching physicochemical properties on protein surfaces. Functional groups of the protein surface residues, such as aromatic rings, hydroxyl groups, or amide groups, are identified, and each is assigned a specific physicochemical property. The set of physicochemical properties as points in space are represented as a graph, from which subgraphs are created. Two compared subgraphs can be transformed into a product graph, in which the algorithm then finds a maximum clique[25] that corresponds to the maximum agreement between the three-dimensional patterns of the compared sets of physicochemical properties. Alignment scores are assigned and subsequently normalized into the *z*-scores. Similar structure sites with the highest *z*-scores are collected and their ligands transposed to the query protein. Ligands are clustered, and the space occupied by the ligands in each cluster is defined as the protein binding sites.

We have developed the ProBiS plugin, which, given a protein structure as input, allows prediction of its binding sites and potential ligands. It is available as a plugin for the widely used PyMOL Molecular Graphics[26] and UCSF Chimera[27] molecular visualization programs. It enables viewing of predicted binding sites and, for each site, its associated family of predicted ligands in three-dimensional graphics. This facilitates their analysis and further use in various applications such as drug repositioning or ligand homology modeling. Binding site prediction computations for proteins in the PDB can be lengthy, and so we have prepared a database of precalculated binding sites. This database resides on our server and is connected to the plugin through the Representational State Transfer (RESTful) API protocol. The plugin allows live computation of binding sites using the ProBiS algorithm[24] on a specially prepared database of all known binding sites and their corresponding ligands from PDB, which is performed on the client computer from the plugin itself.

ProBiS plugin, freely available on our server at http://insilab.org/probis-plugin, is an extension of our earlier ProBiS-ligands approach[28] available at http://probis.cmm.ki.si that predicts protein ligands by searching for structurally similar binding sites and transposition of ligands between these sites. Major

DOI: 10.1021/acs.jmedchem.6b01277
J. Med. Chem. 2016, 59, 11069−11078

improvements in the ProBiS plugin over the earlier approach include:

- ProBiS plugin enables prediction of small molecule ligands and binding sites for all ~290000 protein chains in the PDB, while the ProBiS-ligands approach only enabled prediction of ligands for the 42000 protein chains in the 95% nonredundant PDB.
- The plugin calculates three-dimensional grid models of binding sites that define the size and the shape of the predicted binding sites.
- The new database of binding site comparisons is focused on small ligand binding sites only, while the database used in ProBiS-ligands considered whole protein surfaces. By small ligand we mean synthetic or naturally occurring chemical compound, not peptides, proteins, or other biological macromolecules. Consequently, a database search for similar binding sites is much faster.
- The focused search on the small ligands binding sites enables feasible prediction of ligands' poses in the binding site on the target protein directly applicable in drug repositioning.
- Interactions of the predicted ligands with the binding site residues, including hydrogen bonds and π-stacking interactions, are calculated and visualized.

Results from ProBiS plugin have been assessed experimentally. We applied the plugin to predict ligands for the InhA protein, an enoyl reductase enzyme in the *Mycobacterium tuberculosis* fatty acid biosynthesis pathway and a validated drug discovery target.[29] Our subsequent experimental testing of the predicted ligands revealed micromolar inhibitors of this enzyme with novel scaffolds, highlighting the power of this approach in both target and scaffold hopping. The ProBiS plugin facilitates drug repositioning by helping researchers find novel enzyme inhibitors that, although used in different therapeutic areas, were previously not known to be enoyl reductase inhibitors.

RESULTS AND DISCUSSION

The mycobacterial fatty acid biosynthesis pathway II has been a familiar target for drug discovery and offers an attractive means of achieving selective action with novel antibacterial agents.[30,31] A key enzyme in this pathway is InhA, a NADH-dependent enoyl-acyl carrier protein reductase, currently targeted by the first-line antimycobacterial drug isoniazid. Because of increasing resistance to isoniazid,[32−34] new compounds that target InhA are being sought to assist in treatment of infections caused by resistant strains of *M. tuberculosis*. With the ProBiS plugin, we applied a drug repositioning strategy to identify novel InhA inhibitors. By transposition of ligands found in binding sites of other proteins, which are similar to that of the InhA enzyme but whose protein structures shared approximately 30% sequence identity, we identified three modestly potent InhA inhibitors with novel scaffolds compared to the previously reported InhA inhibitors[35] (see also Literature Review in Experimental Section).

Binding Sites and Ligands Prediction. For the query InhA protein structure (PDB/Chain ID: 4BQP.A),[36] its binding sites and ligands were predicted by the ProBiS plugin (Figure 1). The binding site with the largest volume and the deepest cavity corresponds to the known location of the crystal ligand; almost 600 ligands were predicted to bind to this site. The three remaining binding sites were found to be located on the surface of the protein with only one ligand predicted for each and were discarded. In a search for novel compounds that have not been tested against InhA, we have reviewed the list of predicted ligands in the largest binding site and selected ligands that stem from proteins related, if distantly, to our query protein InhA (Table 1; Supporting Information, Table S1).

Table 1. Structures of the Best Original (PDB) or Analogue (ZINC) Inhibitors, Their Inhibitory Potencies, and Binding Efficiency Indices[b]

Cpd	Original PDB structure (Ligand ID)	Analogue ZINC structure (ZINC ID)	IC_{50} (μM)	BEI[a]
0	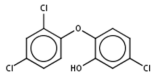 Triclosan	no analogue	0.46 ± 0.06	22
4	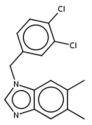 09T	no analogue	10 ± 2	16
7	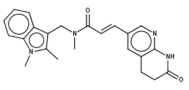 IMJ	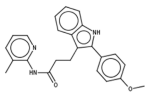 ZINC12515832	62 ± 6	11
8	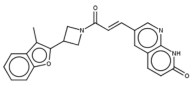 AE6	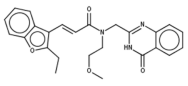 ZINC12890021	14 ± 5	11

[a]Binding-efficiency index is defined as BEI = pIC_{50}/MWT. IC_{50} is in the units of mol/L; MWT is in kDa. [b]Triclosan was used as a positive control.

These represent novel scaffolds and thus opportunities which presumably have not been considered by biochemists. We purchased the PDB compounds whose scaffolds have not been tested against *M. tuberculosis* InhA according to our literature search (see Literature Review in Experimental Section); for PDB compounds that could not be purchased, we performed a similarity search in the ZINC database (http://zinc.docking.org) and purchased the most similar available analogue of the compound. To assess the binding of ZINC analogues to InhA before in vitro tests, we performed comparative docking study of the original PDB compounds and their corresponding ZINC analogues. All the docked ZINC analogues scores were found to be within the AutoDock Vina's standard error (2.8 kcal/mol)[37] of the scores of the original PDB compounds (Supporting Information, Table S2), suggesting that the PDB compounds and the ZINC analogues bind to InhA with about the same affinity and that ZINC analogues are suitable substitutions for the PDB compounds.

Biological Activity. Eight purchased compounds were tested for their inhibitory activity against InhA using a

DOI: 10.1021/acs.jmedchem.6b01277
J. Med. Chem. 2016, 59, 11069−11078

continuous spectrophotometric assay. The original PDB compound could be obtained only for the compound **4**; all others were ZINC analogues. The results are presented as residual activities (RAs) of InhA in the presence of 100 μM of each compound (Supporting Information, Table S1), and for the compounds with RAs > 50%, the IC_{50} values were determined (Table 1). Triclosan was used as a positive control to confirm the suitability of the InhA inhibition assay and was a known inhibitor with which the test compounds could be compared.[38] The inhibitory potency of triclosan in our assay was twice that of previously published values (IC_{50} = 460 ± 60 nM versus IC_{50} = 1000 ± 100 nM).[39] This can be attributed to the different assay conditions.

The most potent inhibitor was found to be 1-(3,4-dichlorobenzyl)-5,6-dimethyl-1*H*-benzo[*d*]imidazole, compound **4** (ligand ID: 09T),[40,41] whose inhibitory IC_{50} is 10 ± 2 μM (Table 1 and Figure 1). For **4**, a mixed inhibition type was observed (Supporting Information, Figure S1) and K_i of 4 ± 1 μM was determined (K_m (DD-CoA) = 31 ± 13 μM; K_m (NADH) = 51 ± 11 μM). These results suggest that **4** inhibits InhA regardless of whether the substrate is present in the binding site or not. Compounds **7** and **8** were ZINC analogues, and notably (*E*)-3-(2-ethylbenzofuran-3-yl)-*N*-(2-methoxyethyl)-*N*-((4-oxo-3,4-dihydroquinazolin-2-yl)methyl)acrylamide (**8**) showed good inhibition of InhA with IC_{50} of 14 ± 5 μM. None of the hits (compounds **4**, **7**, and **8**) were found to be in PAINS or among aggregators.[42] Admittedly, **8** has a Michael acceptor, which could make it reactive in a nonspecific fashion. This is a potential concern, although the presence of the N adjacent to the carbonyl could mitigate the reactivity. Despite having a potency and binding efficiency index (BEI) lower that of than triclosan, compounds **4**, **7**, and **8** have novel scaffolds compared to previously tested InhA inhibitors.[35] In particular, **4**, whose toxicity is not significant against mammalian cells even at a concentration of 10 μM[43] and whose BEI is higher than that of some recently developed rhodanine derivative[44] InhA inhibitors, e.g., the compound **33** with BEI of 11,[45] is a promising candidate for further optimization.

Novel Scaffolds by Enzyme Hopping. The tested compounds are active against distantly related proteins from the same class of enzymes and were repositioned for the InhA enzyme. The most potent inhibitor, compound **4**, is originally an inhibitor of FabI (K_i of 360 nM), an enoyl reductase enzyme from *Francisella tularensis* (PDB ID: 3UIC; 33% sequence identity to InhA, protein structure 4BQP); compound **7** (IMJ) is a FabI inhibitor from *Bacillus subtilis* (3OIG; 30% sequence identity to 4BQP), and **8** (AE6) is a FabI inhibitor from *Escherichia coli* (4JX8; 33% sequence identity to 4BQP). The benzimidazole scaffold of **4**,[41] the indole naphthyridinone scaffold of **7**,[46,47] and the benzofuran naphthyridinone scaffold of **8**[48] are known to be FabI inhibitors but have not been tested as InhA inhibitors; none of the 69 crystal InhA structures in the PDB (>90% seq id to 4BQP) have a cocrystallized ligand similar to **4**, **7**, and **8** and no similar compound is in the set of potential inhibitors of InhA in the DUD-E database.[49] Also, none of these compounds are described as InhA inhibitors. This indicates that the inhibitor sets developed for binding InhA and FabI enzymes fail to overlap. Some inhibitors, such as triclosan, are common to both, but the enzymes, which have about a 30% sequence identity, seem to be too distant for the inhibitors of FabI enzyme to be considered as inhibitors of InhA. This situation will become even more common as the PDB continues to grow: there are currently 763 protein structures in the PDB having about 30% sequence identity to 4BQP, and consequently, it is difficult to manually inspect all these structures and their ligands. The ProBiS plugin is useful in this respect because it lists every ligand that has to date been cocrystallized in similar structures in the PDB, making it easy to find such cross-protein compounds.

LigandRMSD and Experimentally Validated Predictions. Independently from the experimental validation, we investigated how well the predicted ligands can be superimposed on the known crystal ligand (1*S*)-1-(5-{[1-(2,6-difluorobenzyl)-1*H*-pyrazol-3-yl]amino}-1,3,4-thiadiazo-2-yl)-1-(4-methyl-1,3-thiazol-2-yl)ethanol (ligand ID: VMY)[36] of InhA (4BQP.A) using LigandRMSD.[50] We expected ligands with low LigandRMSDs to be more likely to bind to InhA. Therefore, after selecting VMY as reference ligand, a LigandRMSD score was automatically assigned to all the 600 ligands associated with the same binding site. Remarkably, excluding ligands associated with proteins having 100% sequence similarity to the query, LigandRMSD prioritized five of the tested compounds (**1**, **4**, **5**, **6**, and **8** in Supporting Information, Table S1) within the first 10 unique candidates. Moreover, considering all redundant ligands that are suggested by LigandRMSD, the best experimental candidate (**4** in Table 1) was at position 8 (or 3 considering only unique ligands); **5** and **6** (twice the same PDB compound) was ranked first. Out of the first 10 unique ligands recommended by LigandRMSD, five compounds were tested, two of which had confirmed experimentally validated activity (**4** and ZINC analogue of **8**); the others were only available as ZINC analogues and were inactive (**1**, **5**, and **6**). These results suggest that LigandRMSD provides a useful scoring with which to select ligands that feasibly bind to the query protein.

CONCLUSIONS

We present a novel ProBiS plugin for PyMOL and UCSF Chimera molecular graphics programs which predicts binding sites and ligands embedded in an advanced visualization. The developed plugin was applied to the prediction of modestly potent inhibitors with novel scaffolds for a key protein associated with tuberculosis and found three experimentally validated inhibitors, demonstrating the plugin's value in drug discovery research. ProBiS plugin is the first tool that, in an intuitive way and in one place, for a given protein structure, lists every ligand that has to date been cocrystallized in similar proteins deposited in the PDB. Exploration of these ligands before starting the drug development project provides a means to review earlier work and to generate ideas for new compounds from the existing structural data.

EXPERIMENTAL SECTION

Plugin Implementation. The plugin is written in Python, supports the prediction of binding sites and ligands, and allows their visualization. The installation instructions are in the Supporting Information. Each predicted binding site or its ligands become separate objects in PyMOL or Chimera and can be individually styled or colored. A binding site can be viewed as a hexagonal close-packed (HCP) grid of points with 1 Å resolution that spans the volume of the entire family of the corresponding ligands. Predicted ligands are shown in stick representation, and their interactions with the protein, including hydrogen bonds and π-stacking interactions, are visualized using the Protein−Ligand Interaction Profiler (PLIP).[51]

The plugin itself is divided into multiple parts represented as tabs (Figure 2). The "Input tab" contains two subtabs: the first, "PDB Protein" allows fast binding site prediction by consulting a

DOI: 10.1021/acs.jmedchem.6b01277
J. Med. Chem. 2016, 59, 11069−11078

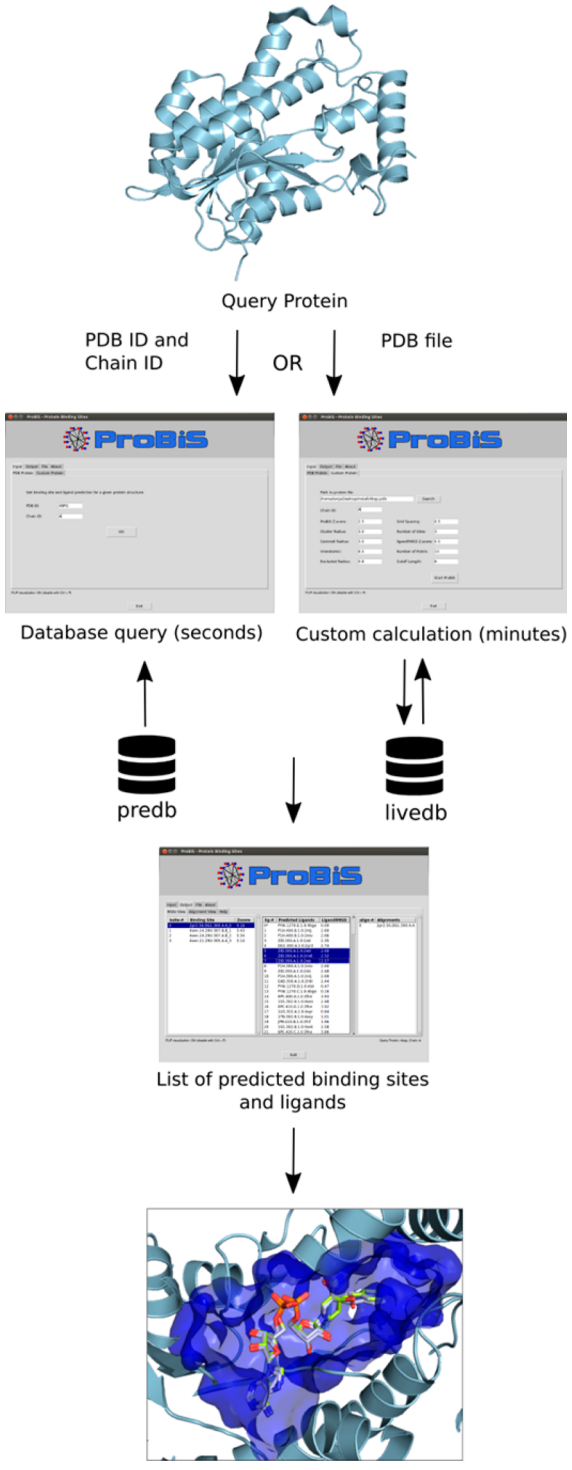

Figure 2. ProBiS plugin input and output. Top left: entering the PDB and Chain identifier retrieves the predicted binding sites and ligands from the "predb". Top right: loading a protein PDB file for live computations using "livedb" with the ProBiS algorithm on client's computer. Middle: list of predicted binding sites (one binding site selected) (left); list of predicted ligands for the chosen binding site (three ligands selected) (middle); the structural alignment to the similar template binding site (right). Bottom: predicted binding site (blue surface) and its predicted ligands (CPK colored sticks) or alignments (not shown) can be visualized as three-dimensional models in the PyMOL viewer.

precalculated database of approximately 290000 existing PDB/Chain identifiers. The second subtab, "Custom Proteins" allows computation with the ProBiS algorithm for any protein structure (including protein models) on the client computer. In the first subtab, the user enters the PDB ID and chain. Subsequently, the selected protein structure is retrieved from the PDB at http://www.rcsb.org, and the corresponding data files that include binding site and ligand predictions (grid and ligand files) can be obtained by querying the RESTful web service on the ProBiS server. The RESTful service is implemented in PHP on an Apache2 web server and enables connection between the database and many plugins worldwide through the HTTP protocol, providing access to the precalculated database of binding site comparisons. In the "Custom Proteins" subtab for custom protein computation, the user is first asked to download and install the binding sites database in a "livedb" directory, together with the ProBiS algorithm specific for the client operating system. Then another interface allows prediction of binding sites and ligands for any PDB file on the client's computer.

The "Output tab" consists of subtabs named "BSite View" and "Alignment View", which allow for alternative views of the results. The "BSite View" presents the list of identified binding sites. Here the user can select one or more binding sites. A list of predicted ligands corresponding to the selected binding sites is shown. By selecting ligand(s), one gets alignments between the query protein and the similar template binding site(s) from which the ligand(s) were transposed. Meanwhile, the "Alignment View" allows the user to explore the data in the opposite direction. The user first sees the list of similar PDB binding sites that were detected using ProBiS; selection of binding site(s) from this list shows ligand(s) that were transposed from this particular template binding site to the query protein. Finally, clicking on a ligand shows its associated predicted binding site on the query protein.

Construction of Binding Sites Databases. For the purposes of this plugin, we constructed two new databases (Figure 3). The "livedb" is a collection of existing binding sites structures and their bound small-molecule ligands extracted from the PDB and can be downloaded to the client computer to enable live computations. The "predb" contains precalculated binding sites for each PDB/Chain identifier pair, enabling fast retrieval of binding sites for existing PDB proteins; it resides on the ProBiS web server. These databases are updated monthly synchronously with the PDB updates. In the following sections, it is explained how they were initially generated.

Step 1. For each protein chain (PDB/Chain identifier) in the April 2016 PDB release,[1] the biological assembly, the presumed biological functional form that contains this chain, was constructed using the rules in the header of the corresponding PDB file. Next, the cocrystallized ligands of the protein chain identified by HETATM records from each biological assembly file was extracted (A-form coordinates), considering only ligands with >7 heavy atoms, where at least one atom is <3 Å from the particular protein chain; nonspecific binders (http://www.russelllab.org/wiki/index.php/Non-specific_ligand-protein_binding) and modified residues denoted by a MODRES code were discarded. From each extracted ligand its binding residues, i.e., protein atoms <5 Å from any ligand atoms, and generated binding site surface files (.srf files) were then obtained using the "extract" command of the ProBiS program.

Step 2. The ~290000 protein chains in the PDB were clustered using a sequence identify cutoff at 100%, resulting in 65924 protein chain clusters. The binding sites obtained in step 1 were then assigned to their associate sequence clusters. Each binding site was assigned to a cluster that contains the protein (identified by PDB/Chain identifier) from which this binding site was extracted.

Step 3. Within each sequence identity cluster, each pair of binding sites was compared in an all-against-all fashion and their pairwise similarity expressed with z-scores was calculated using the ProBiS algorithm.

Step 4. The binding sites within each sequence cluster were then clustered. This second clustering was done solely based on the local structural similarity of binding sites so that similar binding site pairs (with z-score ≥ 2.0) are assigned to the same cluster. Such clustering of binding sites within existing sequence identity clusters ensures that

DOI: 10.1021/acs.jmedchem.6b01277
J. Med. Chem. 2016, 59, 11069−11078

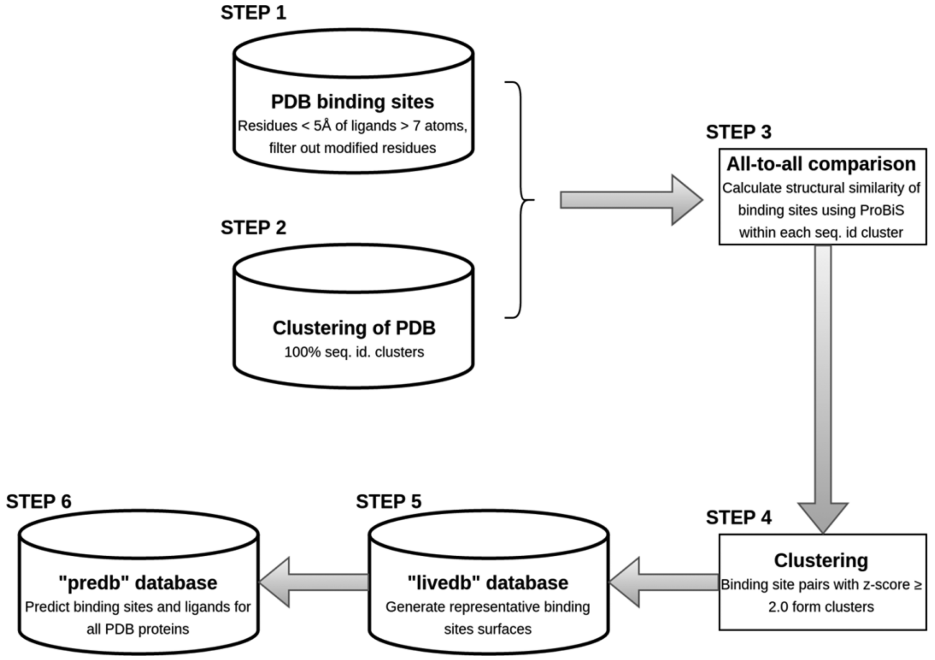

Figure 3. Flow diagram for the generation of the structural databases. The "livedb" template binding sites library and "predb" precalculated binding sites and ligands database.

if a protein has two or more different binding sites, then each one can be assigned to a separate binding site cluster. For each binding site cluster, we then superimposed all of its member sites, their protein coordinates, along with their ligands, which had no influence on the superimposition, onto the representative binding site; representative is arbitrarily chosen as the binding site bound to a ligand with most heavy atoms.

Step 5. The representative binding site surfaces generated in this way (about 35000 surfaces) together with the member ligands transposed to the representative binding site constitute the "livedb" binding site library that can be downloaded through plugins from the "Custom Protein" tab.

Step 6. The precalculated database of binding sites and ligands "predb" was then prepared for each existing protein structural chain in the PDB by comparing that particular chain with the binding site surfaces in the livedb using the ProBiS algorithm. There are >290000 protein chains in the PDB, so to facilitate this task, the approximately 44000 representatives of 90% sequence identity clusters were compared each against the livedb. The remaining nonrepresentative protein chains were compared only to the best scored (z-score $\geq$0) binding sites found for their corresponding cluster representatives. This allowed feasible predictions for each (even nonrepresentative) protein chain in the PDB at a fraction of time needed if all the protein chains are compared to all binding sites of livedb. Finally, only similar binding sites with z-score $\geq$2.5 are considered further. From the obtained alignments for each protein chain, the binding site grids, ligands, and binding sites residues are calculated and saved as the predb library that resides on our server at http://insilab.org/probis-plugin and can be queried using the PDB/Chain identifier from the plugin.

Ligand Clusters and Binding Site Surface Models. An accurate model of a binding site usually follows the contours of the protein surface and covers the volume of all the ligands that bind to this binding site. We first transposed all ligands from the similar binding sites that were found onto the query protein and then clustered them using a fast density-based OPTICS algorithm.[52] Ligands with any two atoms <3 Å apart are clustered together. This results in one or more ligand clusters. We then constructed a 1 Å HCP grid in the space of each ligand cluster so that grid points cover the volume of all the ligands but do not overlap with the protein atoms. Atoms of all ligands reduced to points in space are clustered using a greedy clustering algorithm, and a point representative of each cluster is selected. The resulting representative points are approximately uniformly distributed in space so that the distance between any two points is ∼3 Å. Each point from this reduced set of atoms is then considered a center of a centroid with radius of 4 Å, thus each binding site can have multiple centroids. Finally, a grid is generated by sampling HCP points spaced 1 Å apart that fall within the radius of any of the binding site centroids but do not overlap with any of the protein atoms. The resulting grid point coordinates of the binding sites are saved into a file. By default, a maximum of five binding sites per protein chain are generated and can be displayed in PyMOL or Chimera as point or surface models.

ProBiS Binding Site Comparison. The ProBiS algorithm is used to compare the query protein surface structure with the database of extracted binding sites (livedb). This comparison is done twice: (1) in the process of precalculated database (predb) construction and (2) when the user initiates custom protein comparisons from the PyMOL/Chimera plugin itself.

The livedb database consists of ".srf" files (in SRF format native for ProBiS), each containing a binding site surface patch represented as a graph consisting of a set of vertices and edges connecting them. To define surface residues, a solvent accessible surface is defined by rolling a spherical probe of a radius of 1.4 Å on the van der Waals surface of protein atoms. Residues located within <4 Å of this surface are considered to be surface residues. Vertices in a binding site graph represent the functional groups of surface amino acid residues. A functional group is characterized with five different labels based on its physicochemical properties:[53] hydrogen bond acceptor, donor, aromatic, mixed acceptor/donor, and aliphatic. The query protein graph is constructed similarly; however, to facilitate the computationally intensive maximum clique calculation, we separate this graph into subgraphs of 15 Å in diameter. Each subgraph is centered on one functional group, and all pairs of its vertices are connected by an edge.

In each pairwise comparison, the query protein (broken down into multiple subgraphs) and one binding site graph are compared using the ProBiS algorithm.[24] For a given pair of query protein graph and binding site graph, their product graph is constructed. For two graphs, G_1 and G_2, the vertex set of the Cartesian product graph is defined as $H = V(G_1) \times V(G_2) = \{(u,v)|u \in V(G_1) \wedge v \in V(G_2)\}$. If the physicochemical properties of two vertices of the initial graphs, u and v, are different, the corresponding pair is not considered when generating the product graph. Two vertices of a product graph, (u_1,v_1)

DOI: 10.1021/acs.jmedchem.6b01277
J. Med. Chem. 2016, 59, 11069−11078

and (u_2,v_2), are connected by an edge if and only if the distances between u_1 and v_1 and between u_2 and u_2 differ by <2 Å. The generated product graph is an approximate representation of all possible superpositions of two protein structures. From the generated product graph, we detect its maximum clique,[25] the largest complete subgraph of a graph where all vertices are connected to each other. This represents the largest similar spatial arrangement of functional groups between the two compared proteins (the query protein and the binding site). More than one such similarity can be found for the query protein if the query protein contains two similar binding sites (e.g., two ATP binding sites).

Binding Site Similarity Scores. For an alignment of the query protein surface patch with a binding site from the livedb, we calculated its similarity score using structural similarity and evolutionary similarity.[54] For each alignment, the following four criteria are used to calculate the local alignment score: (1) the difference between the surface angles of the two superimposed patches, (2) the surface patch Root Mean Squared Deviation (RMSD), (3) the corresponding surface patch size, and 4) the *E*-value calculated with the Karlin−Altschul equation.[55] For each surface patch, a surface vector originating from the geometric center of the patch and directed to the perpendicular direction of the surface is generated. If the angle between a pair of surface vectors is larger than 90° or the number of aligned vertices is smaller than 10, the pair is discarded. For the remaining pairs, the alignment score, al_{score}, is calculated as follows:

$$al_{score} = \log\left(\frac{n_{vert} \times \log\left(1 + \frac{1}{e_{value}}\right)}{RMSD}\right)$$

where RMSD is the surface patch RMSD between pairs of superimposed vertices, n_{vert} is the number of aligned vertices, and e_{value} is the alignment expectation value.[54] If RMSD is zero, which happens if two identical binding sites are compared, the al_{score} is set to 100 in order to avoid division by zero. The raw alignment scores are then normalized to the *z*-scores as follows:

$$z\text{-score} = \frac{al_{score} - \mu}{\sigma}$$

where μ and σ are the average and the standard deviation of the alignment scores of all pairs, and the values of μ and σ are 2.0 and 2.2, respectively.

Visualization of Noncovalent Interactions between Ligands and Protein using PLIP. The characterization and display of potential intermolecular contacts provides an important visual control on potential binding of ligands to the query protein. PLIP is a generic rule-based tool for detection and visualization of noncovalent interactions between proteins and their ligands.[51] The calculation of protein−ligand interactions with PLIP is performed remotely on a web server at TU Dresden. Noncovalent contacts from the query protein to one selected ligand are visualized by default and can be toggled using a keyboard shortcut (Ctrl+P). Detected contacts are listed and grouped by type in both PyMOL (in the selection groups) and Chimera (in the PseudoBond panel).

Ligand Similarity Scores. In addition to the *z*-score assigned to a superimposition of two binding sites, the structures of their corresponding cocrystallized ligands may be used as a measure of the similarity of the compared binding sites. The LigandRMSD approach[50] measures how well two bound ligands are aligned by the independent superposition of their binding sites. LigandRMSD is calculated as the difference between the RMSD of an optimal alignment of two ligands, i.e., the optimization of the alignment between two ligands such that RMSD is minimal (RMSD′) and the RMSD of the superposition of the two ligands (RMSD″) according to the alignment of the binding sites: LigandRMSD = RMSD″ − RMSD′. If the two ligands are optimally superimposed, this will translate to LigandRMSD = 0, otherwise LigandRMSD increases as a standard RMSD. The mapping between the atoms of the two ligands is computed as a subgraph isomorphism with OpenBabel.[56] To handle the more common case of nonidentical ligand pairs, the maximum common subgraph between two ligand molecules is computed with SMSD.[57] The ProBiS plugin retrieves LigandRMSDs over a web service hosted at TU Dresden. When the user selects a reference ligand in the plugin, the LigandRMSDs against all other predicted ligands are computed. The reference ligand is marked with asterisk (*) in the list and by default is set to the first ligand in the list of predicted ligands. It can be changed to any other ligand by right-clicking on the mouse or by pressing a keyboard shortcut (Ctrl+R) on the currently selected ligand (see Help tab in the plugin).

Compound Characterization. Compounds used in the subsequent verification experiments were purchased from several vendors and were evaluated without further purification. Additionally, NADH, PIPES, and solvents were obtained from Sigma-Aldrich, Apollo Scientific Ltd., or Merck Millipore and were used without further purification. The substrate 2-*trans*-dodecenoyl-coenzyme A was synthesized and purified according to a previously reported procedure.[58]

^{1}HNMR spectra were recorded in DMSO-d_6, $CDCl_3$, and acetone-d_6 on a Bruker Avance 400 DPX 400 MHz spectrophotometer at 298 K. Chemical shifts are reported in ppm downfield from tetramethylsilane. The coupling constants (J) are in Hz, and the splitting patterns are designated as s, singlet; br s, broad singlet; d, doublet; dd, double doublet; ddd, triple doublet; t, triplet; dt, double triplet; and m, multiplet. ESI-MS mass spectra were recorded on the Advion expression compact mass spectrometer (CMS) at the Faculty of Pharmacy of the University of Ljubljana. The purity of purchased compounds was determined on an Agilent 1100 HPLC system using an Agilent Eclipse Plus C18, 5 μm column (4.6 mm × 150 mm), with a flow rate of 1.0 mL/min, injection volume 5 μL, and detection at 254. The following gradient was applied: 5−70% CH_3CN/H_2O (20 mM phosphate buffer, pH = 7.15) in 15 min, then 5 min at 70% CH_3CN/H_2O (20 mM phosphate buffer, pH = 7.15). The purities of the test compounds used for the biological evaluations were >95%, as determined by HPLC.

InhA Enzymatic Assay. InhA was overexpressed and purified as described previously.[59] The InhA enzymatic activity was measured spectrophotometrically by following NADH oxidation at 340 nm. Kinetic assays were performed at 25 °C for 10 min. Stock solutions (10 mM) of all compounds were prepared in DMSO. The final concentration of DMSO in the assay mixture was 1% v/v. Reactions were initiated by addition of InhA (50 nM) to solutions containing the inhibitor (100 μM), 2-*trans*-dodecenoyl-coenzyme A (DD-CoA, 50 μM), and NADH (100 μM) in 30 mM PIPES, pH 6.8. All compounds were soluble in the conditions of the assay. Control reactions were carried out under the same conditions but without the inhibitor and with 1% v/v DMSO. To exclude possible nonspecific (promiscuous) inhibitors, all compounds were also tested in the presence of Triton X-114 (0.005%).[60] All compounds had comparable activities in the presence and absence of Triton X-114 (Supporting Information, Table S1). The inhibitory activity of each compound was expressed as the percentage of InhA activity inhibition (initial velocity of the reaction) with respect to the control reaction without the inhibitor. All inhibition assays were performed in triplicate with standard deviations within ±10%. IC_{50} values were determined by varying the concentration of inhibitor in the same conditions as described above. Compound **4** was the best inhibitor among those tested. Its inhibition constant (K_i) was determined at different concentrations of one substrate and fixed concentrations of the other under similar conditions as described above. First, the concentration of NADH (100, 300, 500 μM) was varied with a fixed concentration of DD-CoA (50 μM), then the concentration of DD-CoA (100, 300, 500 μM) was varied at fixed concentration of NADH (100 μM). The concentrations used of **4** were 0, 2.5, 5, 10, 17, and 25 μM. Reactions were initiated by addition of InhA (60 nM) to solutions containing the inhibitor, DD-CoA, and NADH in 30 mM PIPES, pH 6.8. All experiments were performed in triplicate. The resulting data were analyzed using the SigmaPlot 12 software[61] and were fitted to software-provided models for competitive, noncompetitive, uncompetitive, and mixed type enzyme inhibition. The mode of inhibition and K_i values were chosen

DOI: 10.1021/acs.jmedchem.6b01277
J. Med. Chem. 2016, 59, 11069−11078

from the best ranking model, as determined by the software. A representative graph depicting the data fit for the best ranking model of inhibition for compound **4** is shown in the Supporting Information (Figure S1).

Literature Review of Existing InhA Scaffolds. A 2012 review of InhA inhibitors[35] mentions the following scaffolds (potency of the best inhibitor [IC_{50} where not stated otherwise], and NAD oxidation state are in parentheses): isoniazid−NAD adducts bisubstrate inhibitors (5 μM), diaryl ethers, most often diphenyl ethers (1 μM, NAD^+),[39,62−64] pyrrolidine carboxamides (low μM, NAD^+),[65] piperazine indoleformamides (100 nM, NAD^+),[66,67] pyrazoles (2.4 μM, NAD^+),[66] arylamides (90 nM, NADH),[68] fatty acids (MIC of 4 μM),[69] and imidazopiperidines (0.24 μM).[70] Except for bisubstrate inhibitors, all form ternary complexes with InhA and the NAD^+ or NADH cofactor; diazaborine (NAD^+)[71] covalently modify the cofactor. Recent inhibitors of InhA not reviewed in ref 35 include: 2-(4-oxoquinazolin-3(4*H*)-yl)-acetamide derivatives (3 μM, NAD^+),[72] methyl-thiazoles (4 nM, prefer NADH-bound form),[36] thienopyrimidines (MIC of 1 μM),[73] tetrahydropyran derivatives (20 nM),[30] thiadiazoles (43 nM, NADH),[31] 4-hydroxy-2-pyridones (0.59 μM, NADH),[74] pyridomycin (K_i of 5 μM, competitive for NADH-binding site),[75] and rhodanine derivatives (2.7 μM, NAD^+).[45]

■ ASSOCIATED CONTENT

Supporting Information

The Supporting Information is available free of charge on the ACS Publications website at DOI: 10.1021/acs.jmedchem.6b01277.

System requirements; ProBiS Plugin Installation; predicted ligands; comparative docking study; comparison of inhibitor structures; hit purity; determination of inhibition constant (PDF)
Ligand cluster 1_4bqpA (PDB)
Compound **4** (PDB)
Compound **7** (PDB)
Compound **8** (PDB)
Molecular formula strings (CSV)

■ AUTHOR INFORMATION

Corresponding Authors

*For D.J.: phone, +386 5 611 76 59; E-mail, dusanka.janezic@upr.si.
*For J.K.: phone, +386 1 476 0273; E-mail, konc@cmm.ki.si.

ORCID

Courtney C. Aldrich: 0000-0001-9261-594X
Sebastian Salentin: 0000-0003-0662-2209

Author Contributions

The manuscript was written through contributions of all authors. All authors have given approval to the final version of the manuscript.

Notes

The authors declare no competing financial interest.

■ ACKNOWLEDGMENTS

We thank Alexander Mestiashvili for deploying the LigandRMSD and PLIP webservices at TU Dresden and Dr. Peter Tonge at Stony Brook University for providing expression plasmid pET15b-*inhA*.

■ ABBREVIATIONS USED

ProBiS, protein binding sites; PAINS, pan assay interference compounds; RESTful API, Representational State Transfer Application Programming Interface; HCP, hexagonal close-packed; PLIP, Protein−Ligand Interaction Profiler

■ REFERENCES

(1) Berman, H. M.; Westbrook, J.; Feng, Z.; Gilliland, G.; Bhat, T. N.; Weissig, H.; Shindyalov, I. N.; Bourne, P. E. The Protein Data Bank. *Nucleic Acids Res.* **2000**, *28* (1), 235−242.
(2) Seco, J.; Luque, F. J.; Barril, X. Binding Site Detection and Druggability Index from First Principles. *J. Med. Chem.* **2009**, *52* (8), 2363−2371.
(3) Schmidtke, P.; Souaille, C.; Estienne, F.; Baurin, N.; Kroemer, R. T. Large-Scale Comparison of Four Binding Site Detection Algorithms. *J. Chem. Inf. Model.* **2010**, *50* (12), 2191−2200.
(4) Konc, J.; Lešnik, S.; Janežič, D. Modeling Enzyme-Ligand Binding in Drug Discovery. *J. Cheminf.* **2015**, *7*, 48.
(5) Shoichet, B. K.; McGovern, S. L.; Wei, B.; Irwin, J. J. Lead Discovery Using Molecular Docking. *Curr. Opin. Chem. Biol.* **2002**, *6* (4), 439−446.
(6) Schneider, G.; Fechner, U. Computer-Based de Novo Design of Drug-like Molecules. *Nat. Rev. Drug Discovery* **2005**, *4* (8), 649−663.
(7) Dean, P. M.; Lloyd, D. G.; Todorov, N. P. De Novo Drug Design: Integration of Structure-Based and Ligand-Based Methods. *Curr. Opin. Drug Discovery Devel.* **2004**, *7* (3), 347−353.
(8) Konc, J.; Hodošček, M.; Ogrizek, M.; Trykowska Konc, J. T.; Janežič, D. Structure-Based Function Prediction of Uncharacterized Protein Using Binding Sites Comparison. *PLoS Comput. Biol.* **2013**, *9* (11), e1003341.
(9) Aubé, J. Drug Repurposing and the Medicinal Chemist. *ACS Med. Chem. Lett.* **2012**, *3* (6), 442−444.
(10) Moriaud, F.; Richard, S. B.; Adcock, S. A.; Chanas-Martin, L.; Surgand, J.-S.; Ben Jelloul, M.; Delfaud, F. Identify Drug Repurposing Candidates by Mining the Protein Data Bank. *Briefings Bioinf.* **2011**, *12* (4), 336−340.
(11) Oprea, T. I.; Nielsen, S. K.; Ursu, O.; Yang, J. J.; Taboureau, O.; Mathias, S. L.; Kouskoumvekaki, I.; Sklar, L. A.; Bologa, C. G. Associating Drugs, Targets and Clinical Outcomes into an Integrated Network Affords a New Platform for Computer-Aided Drug Repurposing. *Mol. Inf.* **2011**, *30* (2−3), 100−111.
(12) Oprea, T. I.; Mestres, J. Drug Repurposing: Far Beyond New Targets for Old Drugs. *AAPS J.* **2012**, *14* (4), 759−763.
(13) Pihan, E.; Colliandre, L.; Guichou, J.-F.; Douguet, D. E-Drug3D: 3D Structure Collections Dedicated to Drug Repurposing and Fragment-Based Drug Design. *Bioinformatics* **2012**, *28* (11), 1540−1541.
(14) Salentin, S.; Haupt, V. J.; Daminelli, S.; Schroeder, M. Polypharmacology Rescored: Protein−ligand Interaction Profiles for Remote Binding Site Similarity Assessment. *Prog. Biophys. Mol. Biol.* **2014**, *116* (2−3), 174−186.
(15) Schneider, G.; Böhm, H.-J. Virtual Screening and Fast Automated Docking Methods. *Drug Discovery Today* **2002**, *7* (1), 64−70.
(16) Knegtel, R. M. A.; Kuntz, I. D.; Oshiro, C. M. Molecular Docking to Ensembles of Protein Structures. *J. Mol. Biol.* **1997**, *266* (2), 424−440.
(17) Steffen, A.; Thiele, C.; Tietze, S.; Strassnig, C.; Kämper, A.; Lengauer, T.; Wenz, G.; Apostolakis, J. Improved Cyclodextrin-Based Receptors for Camptothecin by Inverse Virtual Screening. *Chem. - Eur. J.* **2007**, *13* (24), 6801−6809.
(18) Moro, S.; Deflorian, F.; Bacilieri, M.; Spalluto, G. Ligand-Based Homology Modeling as Attractive Tool to Inspect GPCR Structural Plasticity. *Curr. Pharm. Des.* **2006**, *12* (17), 2175−2185.
(19) Cavasotto, C. N.; Orry, A. J. W.; Murgolo, N. J.; Czarniecki, M. F.; Kocsi, S. A.; Hawes, B. E.; O'Neill, K. A.; Hine, H.; Burton, M. S.; Voigt, J. H.; Abagyan, R. A.; Bayne, M. L.; Monsma, F. J. Discovery of Novel Chemotypes to a G-Protein-Coupled Receptor through Ligand-Steered Homology Modeling and Structure-Based Virtual Screening. *J. Med. Chem.* **2008**, *51* (3), 581−588.

DOI: 10.1021/acs.jmedchem.6b01277
J. Med. Chem. 2016, 59, 11069−11078

(20) Evers, A.; Klebe, G. Ligand-Supported Homology Modeling of G-Protein-Coupled Receptor Sites: Models Sufficient for Successful Virtual Screening. *Angew. Chem., Int. Ed.* **2004**, *43* (2), 248−251.
(21) Ding, Y.; Fang, Y.; Feinstein, W. P.; Ramanujam, J.; Koppelman, D. M.; Moreno, J.; Brylinski, M.; Jarrell, M. GeauxDock: A Novel Approach for Mixed-Resolution Ligand Docking Using a Descriptor-Based Force Field. *J. Comput. Chem.* **2015**, *36* (27), 2013−2026.
(22) Brylinski, M.; Skolnick, J. FINDSITELHM: A Threading-Based Approach to Ligand Homology Modeling. *PLoS Comput. Biol.* **2009**, *5* (6), e1000405.
(23) Haupt, V. J.; Aguilar Uvalle, J. E.; Salentin, S.; Daminelli, S.; Leonhardt, F.; Konc, J.; Schroeder, M. Computational Drug Repositioning by Target Hopping: A Use Case in Chagas Disease. *Curr. Pharm. Des.* **2016**, *22*, 3124−3134.
(24) Konc, J.; Janežič, D. ProBiS Algorithm for Detection of Structurally Similar Protein Binding Sites by Local Structural Alignment. *Bioinformatics* **2010**, *26* (9), 1160−1168.
(25) Konc, J.; Janežič, D. An Improved Branch and Bound Algorithm for the Maximum Clique Problem. *MATCH Commun. Math. Comput. Chem.* **2007**, *58* (5), 569−590.
(26) Delano, W. *The PyMOL Molecular Graphics System*; 2016; http://www.pymol.org (accessed Apr 26, 2016).
(27) Pettersen, E. F.; Goddard, T. D.; Huang, C. C.; Couch, G. S.; Greenblatt, D. M.; Meng, E. C.; Ferrin, T. E. UCSF Chimera–a Visualization System for Exploratory Research and Analysis. *J. Comput. Chem.* **2004**, *25* (13), 1605−1612.
(28) Konc, J.; Janežič, D. ProBiS-Ligands: A Web Server for Prediction of Ligands by Examination of Protein Binding Sites. *Nucleic Acids Res.* **2014**, *42* (W1), W215−W220.
(29) Kinnings, S. L.; Liu, N.; Buchmeier, N.; Tonge, P. J.; Xie, L.; Bourne, P. E. Drug Discovery Using Chemical Systems Biology: Repositioning the Safe Medicine Comtan to Treat Multi-Drug and Extensively Drug Resistant Tuberculosis. *PLoS Comput. Biol.* **2009**, *5* (7), e1000423.
(30) Pajk, S.; Živec, M.; Šink, R.; Sosič, I.; Neu, M.; Chung, C.; Martínez-Hoyos, M.; Pérez-Herrán, E.; Álvarez-Gómez, D.; Álvarez-Ruíz, E.; Mendoza-Losana, A.; Castro-Pichel, J.; Barros, D.; Ballell-Pages, L.; Young, R. J.; Convery, M. A.; Encinas, L.; Gobec, S. New Direct Inhibitors of InhA with Antimycobacterial Activity Based on a Tetrahydropyran Scaffold. *Eur. J. Med. Chem.* **2016**, *112*, 252−257.
(31) Šink, R.; Sosič, I.; Živec, M.; Fernandez-Menendez, R.; Turk, S.; Pajk, S.; Alvarez-Gomez, D.; Lopez-Roman, E. M.; Gonzales-Cortez, C.; Rullas-Triconado, J.; Angulo-Barturen, I.; Barros, D.; Ballell-Pages, L.; Young, R. J.; Encinas, L.; Gobec, S. Design, Synthesis, and Evaluation of New Thiadiazole-Based Direct Inhibitors of Enoyl Acyl Carrier Protein Reductase (InhA) for the Treatment of Tuberculosis. *J. Med. Chem.* **2015**, *58* (2), 613−624.
(32) Gandhi, N. R.; Nunn, P.; Dheda, K.; Schaaf, H. S.; Zignol, M.; van Soolingen, D.; Jensen, P.; Bayona, J. Multidrug-Resistant and Extensively Drug-Resistant Tuberculosis: A Threat to Global Control of Tuberculosis. *Lancet* **2010**, *375* (9728), 1830−1843.
(33) Shah, N. S.; Wright, A.; Bai, G.-H.; Barrera, L.; Boulahbal, F.; Martín-Casabona, N.; Drobniewski, F.; Gilpin, C.; Havelková, M.; Lepe, R.; Lumb, R.; Metchock, B.; Portaels, F.; Rodrigues, M. F.; Rüsch-Gerdes, S.; Van Deun, A.; Vincent, V.; Laserson, K.; Wells, C.; Cegielski, J. P. Worldwide Emergence of Extensively Drug-Resistant Tuberculosis. *Emerging Infect. Dis.* **2007**, *13* (3), 380−387.
(34) Siddiqi, N.; Shamim, M.; Hussain, S.; Choudhary, R. K.; Ahmed, N.; Prachee; Banerjee, S.; Savithri, G. R.; Alam, M.; Pathak, N.; Amin, A.; Hanief, M.; Katoch, V. M.; Sharma, S. K.; Hasnain, S. E. Molecular Characterization of Multidrug-Resistant Isolates of Mycobacterium Tuberculosis from Patients in North India. *Antimicrob. Agents Chemother.* **2002**, *46* (2), 443−450.
(35) Pan, P.; Tonge, P. J. Targeting InhA, the FASII Enoyl-ACP Reductase: SAR Studies on Novel Inhibitor Scaffolds. *Curr. Top. Med. Chem.* **2012**, *12* (7), 672−693.
(36) Shirude, P. S.; Madhavapeddi, P.; Naik, M.; Murugan, K.; Shinde, V.; Nandishaiah, R.; Bhat, J.; Kumar, A.; Hameed, S.; Holdgate, G.; Davies, G.; McMiken, H.; Hegde, N.; Ambady, A.; Venkatraman, J.; Panda, M.; Bandodkar, B.; Sambandamurthy, V. K.; Read, J. A. Methyl-Thiazoles: A Novel Mode of Inhibition with the Potential to Develop Novel Inhibitors Targeting InhA in Mycobacterium Tuberculosis. *J. Med. Chem.* **2013**, *56* (21), 8533−8542.
(37) Trott, O.; Olson, A. J. AutoDock Vina: Improving the Speed and Accuracy of Docking with a New Scoring Function, Efficient Optimization, and Multithreading. *J. Comput. Chem.* **2010**, *31* (2), 455−461.
(38) Parikh, S. L.; Xiao, G.; Tonge, P. J. Inhibition of InhA, the Enoyl Reductase from Mycobacterium Tuberculosis, by Triclosan and Isoniazid. *Biochemistry* **2000**, *39* (26), 7645−7650.
(39) Sullivan, T. J.; Truglio, J. J.; Boyne, M. E.; Novichenok, P.; Zhang, X.; Stratton, C. F.; Li, H.-J.; Kaur, T.; Amin, A.; Johnson, F.; Slayden, R. A.; Kisker, C.; Tonge, P. J. High Affinity InhA Inhibitors with Activity against Drug-Resistant Strains of Mycobacterium Tuberculosis. *ACS Chem. Biol.* **2006**, *1* (1), 43−53.
(40) Mehboob, S.; Hevener, K. E.; Truong, K.; Boci, T.; Santarsiero, B. D.; Johnson, M. E. Structural and Enzymatic Analyses Reveal the Binding Mode of a Novel Series of Francisella Tularensis Enoyl Reductase (FabI) Inhibitors. *J. Med. Chem.* **2012**, *55* (12), 5933−5941.
(41) Hevener, K. E.; Mehboob, S.; Su, P.-C.; Truong, K.; Boci, T.; Deng, J.; Ghassemi, M.; Cook, J. L.; Johnson, M. E. Discovery of a Novel and Potent Class of F. Tularensis Enoyl-Reductase (FabI) Inhibitors by Molecular Shape and Electrostatic Matching. *J. Med. Chem.* **2012**, *55* (1), 268−279.
(42) Baell, J. B.; Holloway, G. A. New Substructure Filters for Removal of Pan Assay Interference Compounds (PAINS) from Screening Libraries and for Their Exclusion in Bioassays. *J. Med. Chem.* **2010**, *53* (7), 2719−2740.
(43) Wilkinson, C.; McPhillie, M. J.; Zhou, Y.; Woods, S.; Afanador, G. A.; Rawson, S.; Khaliq, F.; Prigge, S. T.; Roberts, C. W.; Rice, D. W.; McLeod, R.; Fishwick, C. W.; Muench, S. P. The Benzimidazole Based Drugs Show Good Activity against T. Gondii but Poor Activity against Its Proposed Enoyl Reductase Enzyme Target. *Bioorg. Med. Chem. Lett.* **2014**, *24* (3), 911−916.
(44) Tomašić, T.; Peterlin Mašič, L. Rhodanine as a Scaffold in Drug Discovery: A Critical Review of Its Biological Activities and Mechanisms of Target Modulation. *Expert Opin. Drug Discovery* **2012**, *7* (7), 549−560.
(45) Slepikas, L.; Chiriano, G.; Perozzo, R.; Tardy, S.; Kranjc-Pietrucci, A.; Patthey-Vuadens, O.; Ouertatani-Sakouhi, H.; Kicka, S.; Harrison, C. F.; Scrignari, T.; Perron, K.; Hilbi, H.; Soldati, T.; Cosson, P.; Tarasevicius, E.; Scapozza, L. In Silico Driven Design and Synthesis of Rhodanine Derivatives as Novel Antibacterials Targeting the Enoyl Reductase InhA. *J. Med. Chem.* **2016**, DOI: 10.1021/acs.jmedchem.5b01620.
(46) Seefeld, M. A.; Miller, W. H.; Newlander, K. A.; Burgess, W. J.; DeWolf, W. E.; Elkins, P. A.; Head, M. S.; Jakas, D. R.; Janson, C. A.; Keller, P. M.; Manley, P. J.; Moore, T. D.; Payne, D. J.; Pearson, S.; Polizzi, B. J.; Qiu, X.; Rittenhouse, S. F.; Uzinskas, I. N.; Wallis, N. G.; Huffman, W. F. Indole Naphthyridinones as Inhibitors of Bacterial Enoyl-ACP Reductases FabI and FabK. *J. Med. Chem.* **2003**, *46* (9), 1627−1635.
(47) Kim, S. J.; Ha, B. H.; Kim, K.-H.; Hong, S. K.; Shin, K.-J.; Suh, S. W.; Kim, E. E. Dimeric and Tetrameric Forms of Enoyl-Acyl Carrier Protein Reductase from Bacillus Cereus. *Biochem. Biophys. Res. Commun.* **2010**, *400* (4), 517−522.
(48) Takhi, M.; Sreenivas, K.; Reddy, C. K.; Munikumar, M.; Praveena, K.; Sudheer, P.; Rao, B. N. V. M.; Ramakanth, G.; Sivaranjani, J.; Mulik, S.; Reddy, Y. R.; Narasimha Rao, K.; Pallavi, R.; Lakshminarasimhan, A.; Panigrahi, S. K.; Antony, T.; Abdullah, I.; Lee, Y. K.; Ramachandra, M.; Yusof, R.; Rahman, N. A.; Subramanya, H. Discovery of Azetidine Based Ene-Amides as Potent Bacterial Enoyl ACP Reductase (FabI) Inhibitors. *Eur. J. Med. Chem.* **2014**, *84*, 382−394.
(49) Mysinger, M. M.; Carchia, M.; Irwin, J. J.; Shoichet, B. K. Directory of Useful Decoys, Enhanced (DUD-E): Better Ligands and Decoys for Better Benchmarking. *J. Med. Chem.* **2012**, *55* (14), 6582−6594.

DOI: 10.1021/acs.jmedchem.6b01277
J. Med. Chem. 2016, 59, 11069−11078

(50) Haupt, V. J.; Daminelli, S.; Schroeder, M. Drug Promiscuity in PDB: Protein Binding Site Similarity Is Key. *PLoS One* **2013**, *8* (6), e65894.
(51) Salentin, S.; Schreiber, S.; Haupt, V. J.; Adasme, M. F.; Schroeder, M. PLIP: Fully Automated Protein−ligand Interaction Profiler. *Nucleic Acids Res.* **2015**, *43*, W443−W447.
(52) Ankerst, M.; Breunig, M. M.; Kriegel, H.-P.; Sander, J. OPTICS: Ordering Points to Identify the Clustering Structure. In *Proceedings of the 1999 ACM SIGMOD International Conference on Management of Data*; ACM: New York, 1999; pp 49−60.
(53) Schmitt, S.; Kuhn, D.; Klebe, G. A New Method to Detect Related Function Among Proteins Independent of Sequence and Fold Homology. *J. Mol. Biol.* **2002**, *323* (2), 387−406.
(54) Konc, J.; Česnik, T.; Konc, J. T.; Penca, M.; Janežič, D. ProBiS-Database: Precalculated Binding Site Similarities and Local Pairwise Alignments of PDB Structures. *J. Chem. Inf. Model.* **2012**, *52* (2), 604−612.
(55) Karlin, S.; Altschul, S. F. Methods for Assessing the Statistical Significance of Molecular Sequence Features by Using General Scoring Schemes. *Proc. Natl. Acad. Sci. U. S. A.* **1990**, *87* (6), 2264−2268.
(56) O'Boyle, N. M.; Morley, C.; Hutchison, G. R. Pybel: A Python Wrapper for the OpenBabel Cheminformatics Toolkit. *Chem. Cent. J.* **2008**, *2*, 5.
(57) Rahman, S.; Bashton, M.; Holliday, G. L.; Schrader, R.; Thornton, J. M. Small Molecule Subgraph Detector (SMSD) Toolkit. *J. Cheminf.* **2009**, *1*, 12.
(58) Košak, U.; Kovač, A.; Gobec, S. One-Pot Synthesis of β-Keto Esters and Preparation of 3-Ketopalmitoyl-CoA. *Synlett* **2012**, *23* (11), 1609−1612.
(59) Parikh, S.; Moynihan, D. P.; Xiao, G.; Tonge, P. J. Roles of Tyrosine 158 and Lysine 165 in the Catalytic Mechanism of InhA, the Enoyl-ACP Reductase from Mycobacterium Tuberculosis. *Biochemistry* **1999**, *38* (41), 13623−13634.
(60) McGovern, S. L.; Helfand, B. T.; Feng, B.; Shoichet, B. K. A Specific Mechanism of Nonspecific Inhibition. *J. Med. Chem.* **2003**, *46* (20), 4265−4272.
(61) *SigmaPlot*; Systat Software Inc: San Jose, CA.
(62) Delaine, T.; Bernardes-Génisson, V.; Quémard, A.; Constant, P.; Meunier, B.; Bernadou, J. Development of isoniazid−NAD Truncated Adducts Embedding a Lipophilic Fragment as Potential Bi-Substrate InhA Inhibitors and Antimycobacterial Agents. *Eur. J. Med. Chem.* **2010**, *45* (10), 4554−4561.
(63) am Ende, C. W.; Knudson, S. E.; Liu, N.; Childs, J.; Sullivan, T. J.; Boyne, M.; Xu, H.; Gegina, Y.; Knudson, D. L.; Johnson, F.; Peloquin, C. A.; Slayden, R. A.; Tonge, P. J. Synthesis and in Vitro Antimycobacterial Activity of B-Ring Modified Diaryl Ether InhA Inhibitors. *Bioorg. Med. Chem. Lett.* **2008**, *18* (10), 3029−3033.
(64) Kanetaka, H.; Koseki, Y.; Taira, J.; Umei, T.; Komatsu, H.; Sakamoto, H.; Gulten, G.; Sacchettini, J. C.; Kitamura, M.; Aoki, S. Discovery of InhA Inhibitors with Anti-Mycobacterial Activity through a Matched Molecular Pair Approach. *Eur. J. Med. Chem.* **2015**, *94*, 378−385.
(65) Lu, X.-Y.; Chen, Y.-D.; Jiang, Y.-J.; You, Q.-D. Discovery of Potential New InhA Direct Inhibitors Based on Pharmacophoreand 3D-QSAR Analysis Followed by in Silico Screening. *Eur. J. Med. Chem.* **2009**, *44* (9), 3718−3730.
(66) Kuo, M. R.; Morbidoni, H. R.; Alland, D.; Sneddon, S. F.; Gourlie, B. B.; Staveski, M. M.; Leonard, M.; Gregory, J. S.; Janjigian, A. D.; Yee, C.; Musser, J. M.; Kreiswirth, B.; Iwamoto, H.; Perozzo, R.; Jacobs, W. R.; Sacchettini, J. C.; Fidock, D. A. Targeting Tuberculosis and Malaria through Inhibition of Enoyl Reductase; Compound Activity and Structural Data. *J. Biol. Chem.* **2003**, *278* (23), 20851−20859.
(67) Chollet, A.; Mori, G.; Menendez, C.; Rodriguez, F.; Fabing, I.; Pasca, M. R.; Madacki, J.; Korduláková, J.; Constant, P.; Quémard, A.; Bernardes-Génisson, V.; Lherbet, C.; Baltas, M. Design, Synthesis and Evaluation of New GEQ Derivatives as Inhibitors of InhA Enzyme and Mycobacterium Tuberculosis Growth. *Eur. J. Med. Chem.* **2015**, *101*, 218−235.
(68) He, X.; Alian, A.; Ortiz de Montellano, P. R. Inhibition of the Mycobacterium Tuberculosis Enoyl Acyl Carrier Protein Reductase InhA by Arylamides. *Bioorg. Med. Chem.* **2007**, *15* (21), 6649−6658.
(69) Morbidoni, H. R.; Vilchèze, C.; Kremer, L.; Bittman, R.; Sacchettini, J. C.; Jacobs, W. R., Jr. Dual Inhibition of Mycobacterial Fatty Acid Biosynthesis and Degradation by 2-Alkynoic Acids. *Chem. Biol.* **2006**, *13* (3), 297−307.
(70) Wall, M. D.; Oshin, M.; Chung, G. A. C.; Parkhouse, T.; Gore, A.; Herreros, E.; Cox, B.; Duncan, K.; Evans, B.; Everett, M.; Mendoza, A. Evaluation of N-(Phenylmethyl)-4-[5-(Phenylmethyl)-4,5,6,7-Tetrahydro-1H-imidazo[4,5-C]pyridin-4-Yl]benzamide Inhibitors of Mycobacterium Tuberculosis Growth. *Bioorg. Med. Chem. Lett.* **2007**, *17* (10), 2740−2744.
(71) Roujeinikova, A.; Sedelnikova, S.; de Boer, G.-J.; Stuitje, A. R.; Slabas, A. R.; Rafferty, J. B.; Rice, D. W. Inhibitor Binding Studies on Enoyl Reductase Reveal Conformational Changes Related to Substrate Recognition. *J. Biol. Chem.* **1999**, *274* (43), 30811−30817.
(72) Pedgaonkar, G. S.; Sridevi, J. P.; Jeankumar, V. U.; Saxena, S.; Devi, P. B.; Renuka, J.; Yogeeswari, P.; Sriram, D. Development of 2-(4-Oxoquinazolin-3(4H)-Yl)acetamide Derivatives as Novel Enoyl-Acyl Carrier Protein Reductase (InhA) Inhibitors for the Treatment of Tuberculosis. *Eur. J. Med. Chem.* **2014**, *86*, 613−627.
(73) Vilchèze, C.; Baughn, A. D.; Tufariello, J.; Leung, L. W.; Kuo, M.; Basler, C. F.; Alland, D.; Sacchettini, J. C.; Freundlich, J. S.; Jacobs, W. R. Novel Inhibitors of InhA Efficiently Kill Mycobacterium Tuberculosis under Aerobic and Anaerobic Conditions. *Antimicrob. Agents Chemother.* **2011**, *55* (8), 3889−3898.
(74) Manjunatha, U. H.; Rao, S. P. S.; Kondreddi, R. R.; Noble, C. G.; Camacho, L. R.; Tan, B. H.; Ng, S. H.; Ng, P. S.; Ma, N. L.; Lakshminarayana, S. B.; Herve, M.; Barnes, S. W.; Yu, W.; Kuhen, K.; Blasco, F.; Beer, D.; Walker, J. R.; Tonge, P. J.; Glynne, R.; Smith, P. W.; Diagana, T. T. Direct Inhibitors of InhA Are Active against Mycobacterium Tuberculosis. *Sci. Transl. Med.* **2015**, *7* (269), 269ra3.
(75) Hartkoorn, R. C.; Sala, C.; Neres, J.; Pojer, F.; Magnet, S.; Mukherjee, R.; Uplekar, S.; Boy-Röttger, S.; Altmann, K.-H.; Cole, S. T. Towards a New Tuberculosis Drug: Pyridomycin - Nature's Isoniazid: Pyridomycin Targets InhA. *EMBO Mol. Med.* **2012**, *4* (10), 1032−1042.

DOI: 10.1021/acs.jmedchem.6b01277
J. Med. Chem. 2016, 59, 11069−11078